Journal of ELECTRONIC MATERIALS
https://doi.org/10.1007/s11664-017-5950-6

Synthesis, Optical and Photoluminescence Properties of Cu-Doped Zno Nano-Fibers Thin Films: Nonlinear Optics

V. GANESH,[1] G.F. SALEM,[2] I.S. YAHIA,[1,2,4,5,6,7] and F. YAKUPHANOGLU[3]

1.—Advanced Functional Materials and Optoelectronic Laboratory (AFMOL), Department of Physics, Faculty of Science, King Khalid University, P.O. Box 9004, Abha, Saudi Arabia. 2.—Nanoscience Laboratory for Environmental and Bio-medical Applications (NLEBA), Semiconductor Lab., Thin Film Lab, Department of Physics, Faculty of Education, Ain Shams University, Roxy, Cairo 11757, Egypt. 3.—Department of Physics, Faculty of Science, Firat University, Elazig, Turkey. 4.—Nano-Science and Semiconductor Labs, Department of Physics, Faculty of Education, Ain Shams University, Roxy, Cairo, Egypt. 5.—e-mail: dr_isyahia@yahoo.com. 6.—e-mail: ihussein@kku.edu.sa. 7.—e-mail: isyahia@gmail.com

Different concentrations of copper-doped zinc oxide thin films were coated on a glass substrate by sol–gel/spin-coating technique. The structural properties of pure and Cu-doped ZnO films were characterized by different techniques, i.e., atomic force microscopy (AFM), photoluminescence and UV–Vis-NIR spectroscopy. The AFM study revealed that pure and doped ZnO films are formed as nano-fibers with a granular structure. The photoluminescence spectra of these films showed a strong ultraviolet emission peak centered at 392 nm and a strong blue emission peak cantered at 450 nm. The optical band gap of the pure and copper-doped ZnO thin films calculated from optical transmission spectra (3.29–3.23 eV) were found to be increasing with increasing copper doping concentration. The refractive index dispersion curve of pure and Cu-doped ZnO film obeyed the single-oscillator model. The optical dispersion parameters such as E_o, E_d, and n_∞^2 were calculated. Further, the nonlinear refractive index and nonlinear optical susceptibility were also calculated and interpreted.

Key words: Cu-doped ZnO, nano-fibers, sol–gel/spin-coating method, AFM, photo-luminescence, optical dispersion parameters, nonlinear optics

INTRODUCTION

Zinc oxide (ZnO) is an excellent *p*-type material of the II–VI group, possessing versatile applications in the optoelectronic semiconductor industries. It is also useful in exciton-related optical devices[1] due to its wide band gap (3.37 eV), high excitonic binding energy (60 meV),[2] high transmittance and good electrical conductivity.[3] These specific properties have also attracted many device makers in the field of microelectronic, ceramics and optoelectronic laser applications.[4–11] Hence, in order to deal with such critical applications of this excellent material, understanding its physical as well as electrical properties with different conditions are very important for tailoring and choosing the exact preparation parameters of the material.

It is well reported in the literature that the addition of metallic dopants alter the various physical properties of pure semiconductor material.[12,13] Many researchers have been trying to improve the physical and electrical properties of ZnO with the addition of different dopants and by varying deposition parameters.[12] For this purpose, they have used different dopants like Al, Mg, Ga,[14–16] Co,[17] and Cu.[18] Among all the dopants, copper is a most suitable dopant for luminescence properties, and it is considered as a rapid diffusing material in the ZnO structure. This fast diffusing nature of Cu into

(Received January 17, 2017; accepted November 10, 2017)

Published online: 05 December 2017

the ZnO matrix may change the physical and electronic properties of the material and provide a localized impurity level for band gap engineering applications.[19–21]

Different types of deposition methods have been discussed by many researchers on pure and doped ZnO thin films. These methods are vapor deposition (CVD),[22] RF magnetron sputtering,[23] molecular beam epitaxial (MBE),[24] pulsed laser deposition (PLD),[25] spray pyrolysis,[26] the filtered cathodic vacuum arc method,[27] inductively coupled plasma-enhanced physical vapor deposition (ICP-PVD)[28] and the sol–gel method.[29] Sol–gel/spin-coating is the most widely used of the different preparation methods due to its low cost and controlled monitoring nature for the preparation of high-quality thin films.[30–32] Owing to these important features,this work presents the preparation of pure and Cu-doped ZnO thin films with different molar ratios by sol–gel/spin coating technique at low temperature. Further, to understand the influence of Cu on pure ZnO thin films, various characterization techniques were employed i.e., AFM, photoluminescence and UV–Vis-NIR studies and the observed results were compared with the available literature. These results are discussed in their relevant sections.

EXPERIMENTAL

Synthesis of Nano-Structured Cu-Doped ZnO Thin Films

In the present work, pure and different molar concentrations of (0.1%, 0.2%, 0.5%, and 1%) Cu-doped ZnO thin films were deposited by sol–gel/spin coating technique. Initially, 0.2 M zinc acetate dihydrate ($(CH_3COO)_2Zn2H_2O$) was dissolved in the solvent of 2-methoxyethanol (MTE) and a stabilizer of mono-ethanolamine (MEA) slowly added to it. After that, the precursor solution was continuously stirred with a magnetic stirrer for 2 h at 60°C to form a transparent and homogeneous sol. To grow Cu-doped films, 0.2 M copper nitrate ($Cu(NO_3)_2$) with different percentages (0.1%, 0.2%, 0.5%, and 1%) were dissolved in MTE followed by the addition of the stabilizer (MEA) under continuous stirring for the same time and temperature as the pure sample. After the formation of the sol, both pure and doped samples were kept for 24 h in the dark to obtain a homogeneous gel. In order to get high-quality and transparent thin films, glass substrates were thoroughly cleaned by various solutions and dried under nitrogen flow. In the second step, homogeneous and high-quality films were deposited on the glass substrates using a spin-coater with a speed of 3000 rpm for 30 s. After the completion of the spin-coating process, the films were dried at 150°C on a hot plate to evaporate undesired organic solvents. The same process was repeated ten times for each solution to obtain uniform thicknesses. Further, all the films were annealed at 450°C for 1 h in a tube furnace.

Characterization Techniques

The prepared thin films were subjected to the AFM technique (Park system XE-100E) in order to study the thicknesses and microstructure of the pure and doped films. The thicknesses of the pure and Cu-doped samples were found to be 212 nm, 201 nm, 218 nm, 213 nm and 225 nm for pure and doped ZnO thin films, respectively. The photoluminescence (PL) spectra of the samples were recorded by a fluorescence spectrophotometer (LS-45) with an excitation wavelength of 325 nm. The optical absorbance, transmittance and reflectance of these samples were measured by using a Shimadzu UV–VIS-NIR 3600 spectrophotometer in the wavelength range 300–800 nm. Further, various linear and nonlinear optical parameters of these samples were also calculated using the optical data.

RESULTS AND DISCUSSION

Surface Morphology Studies

Figure 1a–e shows the AFM images of the pure and Cu-doped ZnO samples. It can be seen from these micrographs that the pure and doped samples are exhibiting nano-fiber growth with a granular structure. The diameter of the observed nano-fibers is varying with the doping concentration of Cu. The reason for this type of trend is due to the slightly higher radius of Cu compared to Zn atoms which creates an interstitial dopant position in the ZnO matrix.[4,33] The surface roughness values were calculated from AFM micrographs and the values found to be 72.15 nm, 74.78 nm, 71.22 nm, 69.59 nm, and 73.75 nm, respectively. These results indicate that the films have high roughness values due to the thickness of the nano-fibers and the surface defects.

Photoluminescence Study

Figure 2 shows the PL spectra of the pure and Cu-doped ZnO samples. From this study, the intensity of two emission bands decreases with increasing Cu concentration, and the maximum value is found for pure ZnO.[34] The pure and doped samples show an intense ultraviolet (UV) emission peak centered at 392 nm and a strong blue emission peak centered at 450 nm.[13,35,36] The peak at 392 nm is due to the recombination of bound excitons and the peak at 450 nm is attributed due to the presence of intrinsic defects (vacancies and interstitials) and doping concentrations.[37,38] Furthermore, the decrease of PL intensity in the Cu-doped films compared to that of the pure material is attributed to the separation of charge carriers rather than their interactions. Hence, from the present study, it is concluded that the Cu is showing an observable effect on the PL properties of pure ZnO films.

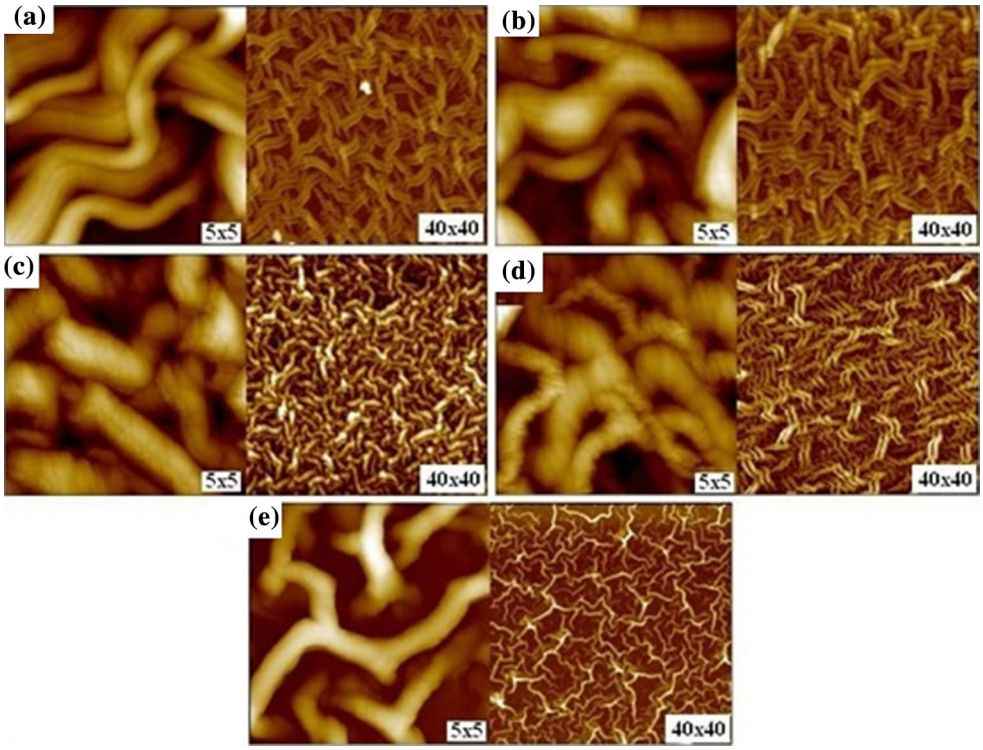

Fig. 1. 2D AFM images of pure and Cu-doped ZnO samples: (a) pure ZnO (b) 0.1% Cu (c) 0.2% Cu (d) 0.5% Cu and (e) 1% Cu.

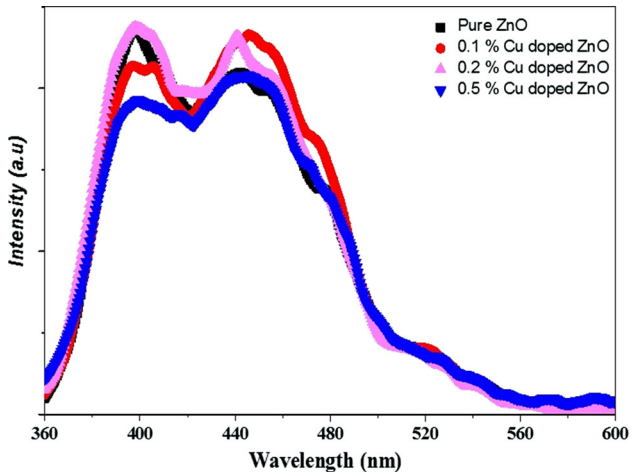

Fig. 2. Photoluminescence spectra of undoped and 0.1%, 0.2%, 0.5% Cu-doped ZnO films.

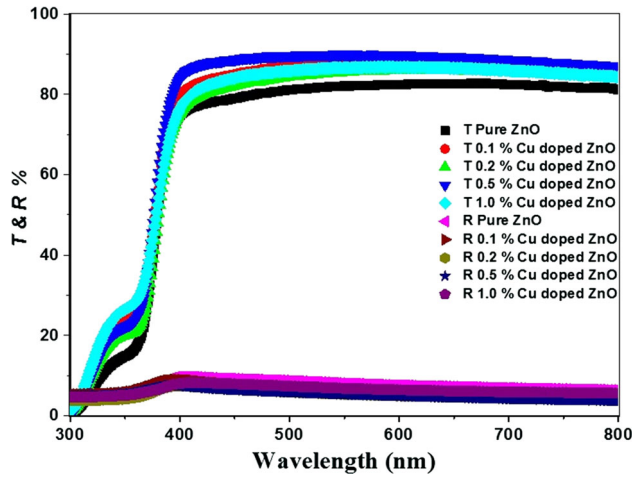

Fig. 3. Transmittance and reflectance spectra of undoped and 0.1%, 0.2%, 0.5% Cu-doped ZnO films.

Optical Properties of Pure and Cu-Doped Nano-ZnO Thin Films

Figure 3 shows the transmittance $T(\lambda)$ and reflectance $R(\lambda)$ spectra of the present samples assessed in the range of 300–800 nm. From these studies, the band edge of the pure and Cu-doped samples was observed at 382–294 nm and found to be decreasing with increasing Cu concentration, indicating the substitution of Cu ions in the ZnO matrix.[33]

The reflectance $R(\lambda)$, n and k are calculated from the Fresnel formula[39] by:

$$R = \frac{(n-1)^2 + k^2}{(n+1)^2 + k^2}, \tag{1}$$

where n is the refractive index and k is the absorption index (extinction coefficient) determined by $k = \alpha\lambda/4\pi$. By solving the above equation using the algebraic functions, the n is given as[39]:

$$n = \left(\frac{1+R}{1-R}\right) + \sqrt{\frac{4R}{(1-R)^2} - k^2}, \tag{2}$$

Next, the k values of the pure and Cu-doped ZnO films are shown in Fig. 4a and b. From Fig. 4a, the refractive index has two regions: the first one is in the lower wavelength region, in which the refractive index is increasing with increasing wavelength (i.e., anomalous dispersion), while in the second region, it is decreasing with increasing wavelength (i.e., normal dispersion). The reason for the increasing refractive index in the lower wavelength region is explained due to more absorption of radiation by the addition of Cu in the ZnO structure. Similarly, the decreasing nature at the higher wavelength is attributed to the influence of band levels. The dispersion and gradual decreasing nature of k is attributed to increases in the doping concentration which increases the impurities in the host material, which in turn acts as scattering centers for the interaction of wavelength. The same phenomenon is also observed by many groups in the cases of Al-, Mg-, Ni- and Ti-doped ZnO structures.[39–41] The band gap is calculated from Tauc's formula[42]:

$$ahu = A(hu - Eg)^m, \tag{3}$$

where α, A, h, are constants, and have their usual meanings,[42] E_g is the optical band gap, and υ is the photon frequency. The optical band gap values of these films are calculated from $(\alpha h\upsilon)^2$ versus $(h\upsilon)$ plots (Fig. 5), and the results are tabulated in Table I. From these plots, the band gap values are found to be decreasing with increasing Cu concentration, which could be attributed to the substitution of Cu ions in the ZnO structure causing exchange of ions in the conduction band and the valence band which eventually results in the band gap narrowing effect due to Burstein–Moss shift.[33] A similar trend has been observed in pure and Cu-doped ZnO thin films in previous reports.[20,43–45]

The optical band gap and optical transition relationship is given by the Urbach tail process. The width of the band tail can be measured from Pankove's expression[46]:

$$a(hu) = AE_u^{3/2}\exp\,(hu/E_u), \tag{4}$$

where E_u is a parameter which describes the width of the localized state in the band gap produced from the oxygen defects, α is the absorption coefficient; A is a constant and $h\upsilon$ is the photon energy of light. The semi-logarithm plots of α against the photon energy are shown in Fig. 6. The obtained values of the empirical parameter E_u are tabulated in Table I. From these values, the pure ZnO film has the minimum width of the tails, and increases with doping concentration.[47,48] The reason for the increasing E_u values in the present study provides the information of an additional number of defects which are introduced due to doping in the pure ZnO matrix. A similar type of results was observed in earlier reports on Cu-doped ZnO thin films.[49]

There are dfferent dispersion formulae available in the literature to calculate the refractive index,

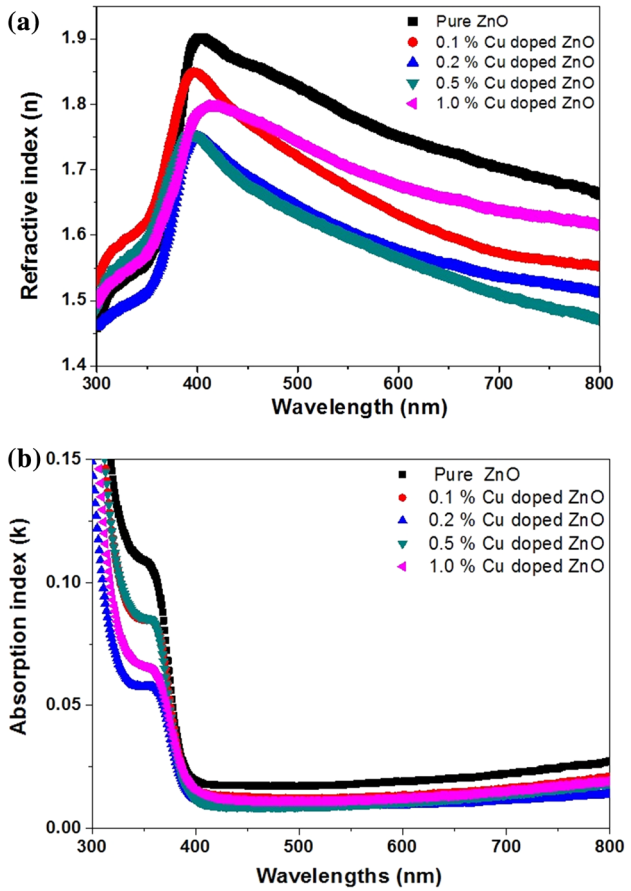

Fig. 4. (a) Refractive index (n), (b) absorption index (k) of undoped and 0.1%, 0.2%, 0.5% Cu-doped ZnO films.

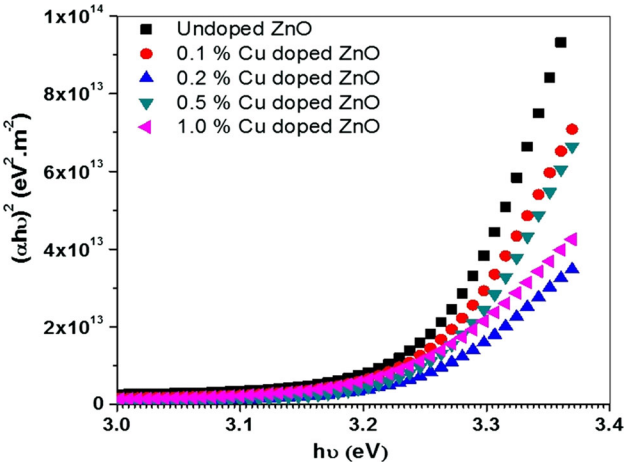

Fig. 5. Plotting of $(\alpha h\upsilon)^2$ versus $h\upsilon$ of undoped and 0.1%, 0.2%, 0.5% Cu-doped ZnO films.

but the most relaible method is the DiDomenico and Wemple expression[50] to fit the exact values of the refractive index for a broad range of frequencies. Hence, we used the same expression for the pure and Cu-doped ZnO thin films. The relationship is as follows:

Table I. Optical band gap and optical dispersion parameters of undoped and Cu-doped ZnO films

	Band gap	Dispersion parameters			
Samples	E_g, (eV)	(E_u), (meV)	$((E_0)$, (eV)	(E_d), (eV)	$\varepsilon_i = n_\infty^2$
Undoped ZnO	3.29	105	5.06	12.35	2.92
0.1% Cu-doped ZnO	3.28	137.5	3.91	8.16	2.50
0.2% Cu-doped ZnO	3.27	140	3.83	7.41	2.32
0.5% Cu-doped ZnO	3.25	142.85	3.68	6.79	3.27
1.0% Cu-doped ZnO	3.23	171.05	4.29	9.3	2.02

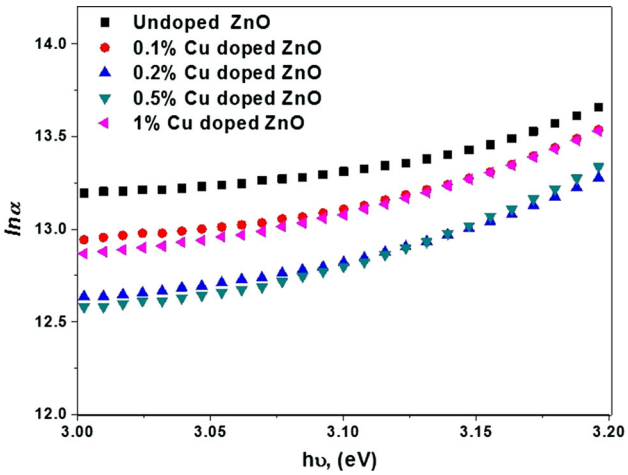

Fig. 6. Plots of $ln\alpha$ versus $h\upsilon$ of undoped and 0.1%, 0.2%, 0.5% Cu-doped ZnO films.

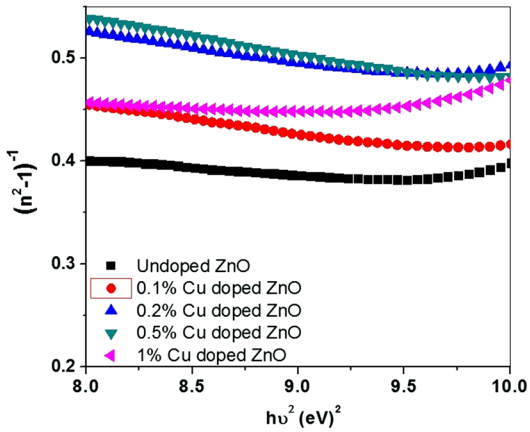

Fig. 7. Plots of $(n^2 - 1)^{-1}$ versus $(h\upsilon)^2$ of undoped and 0.1%, 0.2%, 0.5% Cu-doped ZnO films.

$$n^2 = 1 + \frac{E_d E_0}{E_0^2 - (h\upsilon)^2}, \tag{5}$$

where n is the refractive index, E_o is the single-oscillator energy for electronic transitions, and E_d is the dispersion energy for interband optical transitions. The values of the above-mentioned constants were measured from plots of $(n^2 - 1)^{-1}$ versus $(h\upsilon)^2$ (Fig. 7). The obtained E_o and E_d values suggested that the single-oscillator model is valid to explain the doping effect, and the values found are tabulated in Table I. Further, the parameters E_o and E_d are also related to the imaginary part of the complex dielectric constant $(\varepsilon_i = n^2)$, in which ε_i gives the response of the electronic and optical properties of the present material. The obtained values of ε_i are also given in Table I.

The refractive index of infinite wavelength n_∞ is given by[51]:

$$\frac{n_\infty^2 - 1}{n^2 - 1} = 1 - \left(\frac{\lambda_0}{\lambda}\right)^2, \tag{6}$$

The plots of $(n^2 - 1)^{-1}$ versus λ^{-2} are shown in Fig. 8. The obtained n_∞ values of the pure and Cu-doped samples were tabulated in Table I. From the values of E_g, E_u, and n in Table I, it is obviously understood that the Cu is showing an impact on the pure ZnO matrix and that these values are better than other metallic dopants in ZnO thin films.[39–41,52]

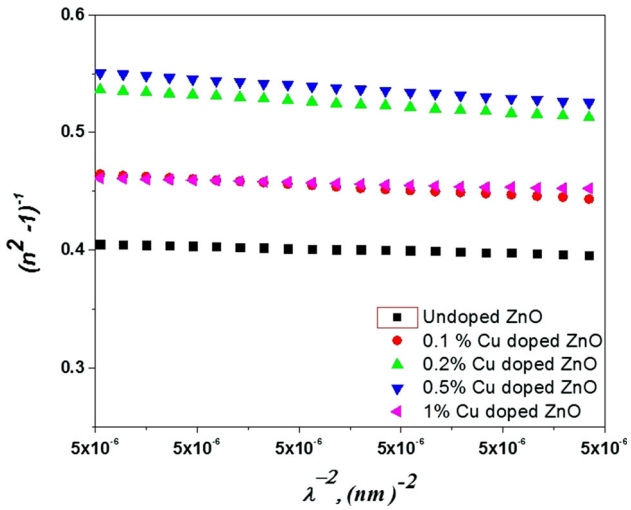

Fig. 8. Plots of $(n^2 - 1)^{-1}$ versus $(\lambda)^{-2}$ of undoped and 0.1%, 0.2%, 0.5% Cu-doped ZnO films.

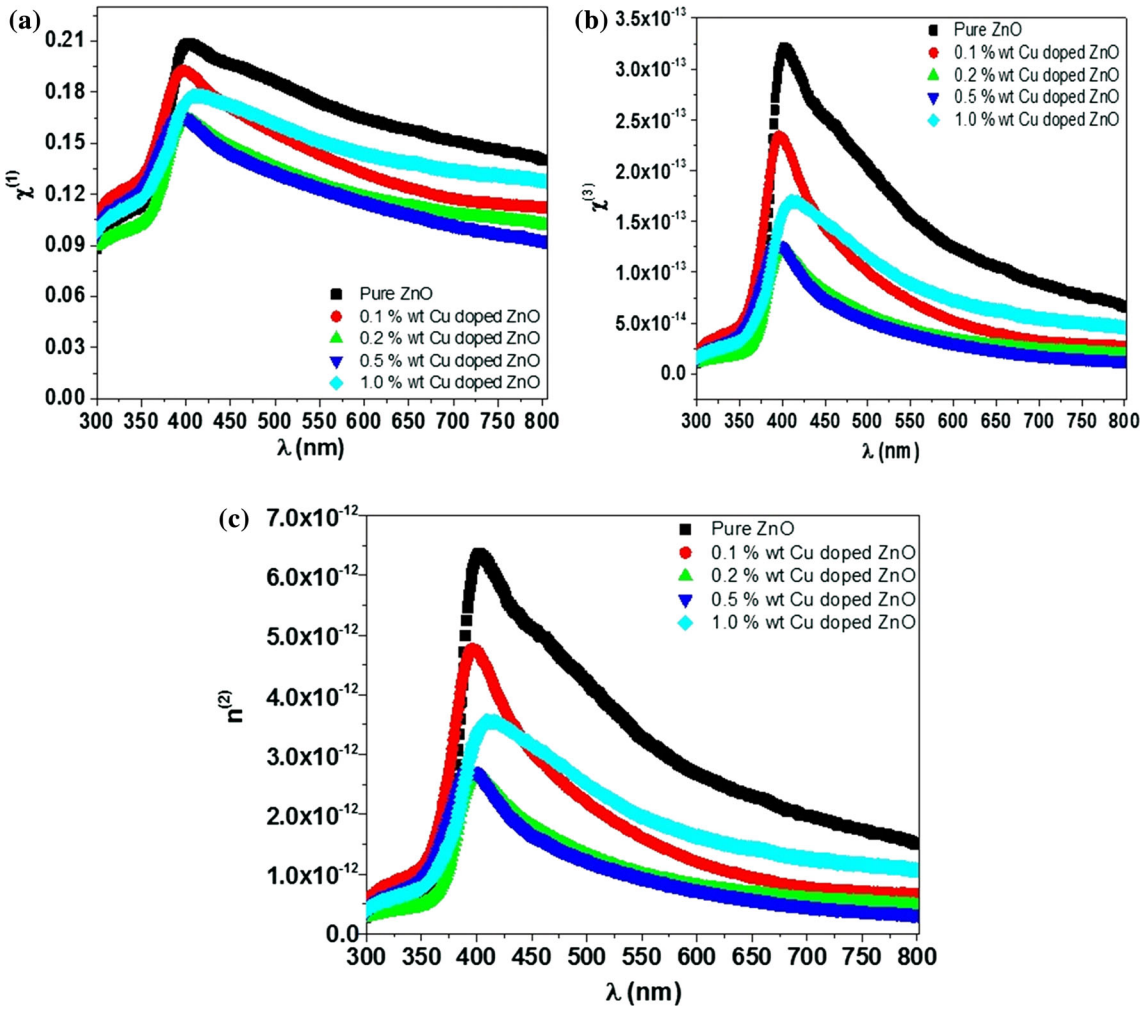

Fig. 9. (a) Linear optical susceptibility $\chi^{(1)}$, (b) third order nonlinear susceptibility $\chi^{(3)}$ of (c) nonlinear refractive index ($n^{(2)}$) of undoped and 0.1%, 0.2%, 0.5% Cu-doped ZnO films.

Table II. Nonlinear optical parameters of reported and present work on ZnO thin films

Samples	$(\chi^{(3)})$	$(\chi^{(3)})$, esu	$(n^{(2)})$, esu
Pure ZnO [60]	0.117	0.313×10^{-13}	1.25×10^{-10}
Co-ZnO [60]	0.13–0.2	$0.489–2.72 \times 10^{-13}$	$1.89–9.11 \times 10^{-10}$
Sn-ZnO [61]	0.1–0.8	$0.5–9.0 \times 10^{-11}$	$0.5–9.0 \times 10^{-10}$
Cu-ZnO (present work)	0.09–0.19	$0.25–2.25 \times 10^{-13}$	$0.25–4.5 \times 10^{-12}$

Nonlinear Optical Parameters

The optical properties like the second- $(\chi^{(2)})$ and third-order susceptibilities $(\chi^{(3)})$ of semiconductor materials play an important role in the interaction of high-intensity laser radiations and produce nonlinear polarizability properties. The nonlinear polarizability (P_{NL}) can be expressed by the following equation[53]:

$$p = \chi^{(1)}E + P_{NL}, \tag{7}$$

where $P_{NL} = \chi^{(2)}E^2 + \chi^{(3)}E^3$, P is polarizability, $\chi^{(1)}$ is the linear optical susceptibility, and $\chi^{(2)}$ and $\chi^{(3)}$ are the second- and third-order nonlinear optical susceptibilities, respectively. The linear refractive index $n(\lambda)$ regarding $n_o(\lambda)$ and E^2 can be represented as follows:

$$n(\lambda) = n_0(\lambda) + n_2(E^2), \tag{8}$$

where the component of $n(\lambda)$ can be written as: $n_o(\lambda) \gg n_2(\lambda)$ i.e. $n(\lambda) = n_o(\lambda)$, and (E^2) is the mean square of electric field. The linear optical susceptibility $\chi^{(1)}$ for a medium can be obtained from the following equation[54]:

$$\chi^{(1)} = (n^2 - 1)/4\pi, \quad (9)$$

The third-order nonlinear susceptibility $\chi^{(3)}$ by linear refractive index $n_o(\lambda)$ and linear optical susceptibility $\chi^{(1)}$ is given as[55–57]:

$$\chi^{(3)} = A\left(\chi^{(1)}\right), \quad (10)$$

From Eqs. 9 and 10, we obtain the following equation:

$$\chi^{(3)} = \frac{A}{(4\pi)^4}\left(n_0^2 - 1\right)^4, \quad (11)$$

The value of the constant (A) value equals 1.7×10^{-10} (for $\chi^{(3)}$ in esu), according to Adair et al.[58] on a different type of material. The nonlinear refractive index can be described by the following simple equation[59]:

$$n^{(2)} = \frac{12\pi\chi^{(3)}}{n_o}, \quad (12)$$

Figure 9a and b shows the variation of linear and third-order optical susceptibilities of the studied thin films. From these plots, it is clear that both the susceptibilities are increasing with the increasing wavelength and attain a constant value at higher wavelength regions. This type of behavior is observed in high crystalline materials of orderly arranged atoms. Hence, in the present studies, the doped samples are showing high susceptibilities compare to the pure material, indicating that the crystalline perfection is increasing with doping concentration. Furthermore, the doping concentration is growing the interaction of the particles with applied wavelength by enhancing the optical susceptibilities. Further, the calculated optical parameters are compared with the earlier reports, and the results ae depicted in Table II.

When dealing with applications in photonic devices, the nonlinear refractive index ($n^{(2)}$) plays a vital role. It is the property that arises due to the interaction of the high-intensity electric field with the incident light. Figure 9c shows the nonlinear refractive index of the pure and doped ZnO samples. The observed trend from the graph is similar to that of nonlinear susceptibility, indicating the high dependence of ($n^{(2)}$) on $\chi^{(3)}$. The calculated values of all the linear and nonlinear optical parameters of pure and Cu-doped ZnO thin films are given in Table II. From these values, it is understood that the present samples are showing higher values than previously studied ZnO thin films in pure and doped forms. Hence, the high value of all these parameters indicates that the present material can replace various other metal oxide thin films for transparent conductive displays and solar cell applications.

CONCLUSIONS

Pure and Cu-doped ZnO thin films with different molar concentrations of 0.1%, 0.2%, 0.5%, and 1% were deposited by the low-cost sol–gel method. The effect of Cu on the pure material has been investigated by surface morphology, PL spectroscopy and various optical analysis through UV–Vis-NIR studies. From AFM studies, the surface roughness values of the pure and Cu-doped ZnO films were analyzed and found to be 72.15 nm, 74.78 nm, 71.22 nm, 69.59 nm and 73.75 nm, respectively. These results suggest that the prepared films have high roughness values due to the nano-fibers growth and the surface defects. The PL spectra confirm the appearance of two characteristics peaks at 392 nm and 450 nm. The optical band gap of the ZnO film is changed with increasing the copper concentration. The refractive index dispersion curve obeys the single-oscillator model and single-oscillator parameters such as E_o, E_d, and n_∞^2 were determined. In the present study, all the observed results are found to be superior to the previous results, indicating that Cu-doped ZnO is a good material for various optoelectronic devices. From the nonlinear refractive index and the optical susceptibility results, the Cu-doped samples show better nonlinear effects than pure ZnO film.

ACKNOWLEDGEMENT

The authors would like to express their gratitude to King Khalid University, Saudi Arabia for providing administrative and technical support with Grant No. R.G.P.2/3/38.

REFERENCES

1. P. Sagar, P.K. Shishodia, R.M. Mehra, H. Okada, A. Wakahara, and A. Yoshida, *J. Lumin.* 126, 800 (2007).
2. F. Benharrats, K. Zitouni, A. Kadri, and B. Gil, *Superlattices Microstruct.* 47, 592 (2010).
3. K. Nakahara, H. Takasu, P. Fons, A. Yamada, K. Iwata, K. Matsubara, R. Hunger, and S. Niki, *Appl. Phys. Lett.* 79, 4139 (2001).
4. B. Kulyk, B. Sahraoui, V. Figà, B. Turko, V. Rudyk, and V. Kapustianyk, *J. Alloys Compd.* 481, 819 (2009).
5. G.M. Ali, S. Singh, and P. Chakrabarti, *J. Electron. Sci. Technol.* 8, 55 (2010).
6. Y.-H. Lin, P.-C. Yang, J.-S. Huang, G.-D. Huang, I.-J. Wang, W. Wen-Hao, M.-Y. Lin, S. Wei-Fang, and C.-F. Lin, *Sol. Energy Mater. Sol. Cells* 95, 2511 (2011).
7. L.J. Mandalapu, F.X. Xiu, Z. Yang, D.T. Zhao, and J.L. Liu, *Appl. Phys. Lett.* 12, 92 (2008).
8. S.S. Badadhe and I.S. Mulla, *Sens. Actuators B Chem.* 156, 943 (2011).
9. K.K. Banger, Y. Yamashita, K. Mori, R.L. Peterson, T. Leedham, J. Rickard, and H. Sirringhaus, *Nat. Mater.* 10, 45 (2011).
10. L. Gao, Q. Li, W. Luan, H. Kawaoka, T. Sekino, and K. Niihara, *J. Am. Ceram. Soc.* 85, 1016 (2002).
11. P. Prepelita, R. Medianu, B. Sbarcea, R. Petronela Prepelita, F. Garoi, and M. Filipescu, *Appl. Surf. Sci.* 256, 1807 (2010).
12. F.J. Haug, Z. Geller, H. Zogg, A.N. Tiwari, and C. Vignali, *J. Vaccum Sci. Technol. A* 19, 171 (2001).
13. X. Peng, X. Jinzhang, H. Zang, B. Wang, and Z. Wang, *J. Lumin.* 128, 297 (2008).
14. J. Ding, H. Chen, X. Zhao, and S. Ma, *J. Phys. Chem. Solids* 71, 346 (2010).
15. Y.W. Heo, S.J. Park, K. Ip, S.J. Pearton, and D.P. Norton, *Appl. Phys. Lett.* 83, 1128 (2003).

16. C. Xu, M. Kim, J. Chun, and D. Kim, *Appl. Phys. Lett.* 86, 133107 (2005).
17. J.H. Kim, H. Kim, D. Kim, Y.E. Ihm, and W.K. Choo, *J. Appl. Phys.* 92, 6066 (2002).
18. S. Eustis, D.C. Meier, M.R. Beversluis, and B. Nikoobakht, *ACS Nano* 2, 368 (2008).
19. D. Paul Joseph and C. Venkateswaran, *J. Atom. Mol. Optic. Phys*. 2011, 270540 (2011).
20. M. Öztas and M. Bedir, *Thin Solid Films* 516, 1703 (2008).
21. Z. Zhang, J.B. Yi, J. Ding, L.M. Wong, H.L. Seng, S.J. Wang, J.G. Tao, G.P. Li, G.Z. Xing, C.H. Alfred Huan, T.C. Sum, and T. Wu, *J. Phys. Chem. C* 112, 9579 (2008).
22. S.T. Tan, B.J. Chen, X.W. Sun, W.J. Fan, H.S. Kwok, X.H. Zhang, and S.J. Chua, *J. Appl. Phys.* 98, 013505 (2005).
23. C.O. Kim, S. Kim, H.T. Oh, S.-H. Choi, Y. Shon, S. Lee, H.N. Hwang, and C.-C. Hwang, *Phys. B Condens. Matter.* 405, 4678 (2010).
24. J.B. Kim, D. Byun, S.Y. Ie, D.H. Park, W.K. Choi, J.-K. Choi, and B. Angadi, *Semicond. Sci. Technol.* 23, 095004 (2008).
25. G. Shukla, *Appl. Phys. A* 97, 115 (2009).
26. E.M. El Jald, V.A. Franiv, A. Belayachi, and M. Abd-Lefdil, *Optik* 124, 6302 (2013).
27. T.S. Herng, S.P. Lau, S.F. Yu, H.Y. Yang, X.H. Ji, J.S. Chen, N. Yasui, and H. Inaba, *J. Appl. Phys.* 99, 086101 (2006).
28. S.-Y. Zhuo, X.-C. Liu, Z. Xiong, J.-H. Yang, and E.-W. Shi, *Solid State Commun.* 152, 257 (2012).
29. T. Saidani, M. Zaabat, M.S. Aida, A. Benaboud, S. Benzitouni, and A. Boudine, *Superlattices Microstruct.* 75, 47 (2014).
30. D. Wang and S. Gao, *J. Alloys Compd.* 476, 925 (2009).
31. I.S. Yahia, G.F. Salem, M.S. Abd El-sadek, and F. Yakuphanoglu, *Superlattices Microstruct.* 64, 178 (2013).
32. C. Aydın, H.M. El-Nasser, F. Yakuphanoglu, I.S. Yahia, and M. Aksoy, *J. Alloys Compd.* 509, 854–858 (2011).
33. D.R. Sahu, *Mater. Sci. Eng., B* 171, 99 (2010).
34. R.-C. Wang and H.-Y. Lin, *Appl. Phys. A* 95, 813 (2009).
35. R. Elilarassi, P.S. Rao, and G. Chandrasekaran, *J. Sol Gel. Sci. Technol.* 57, 101 (2011).
36. U. Choppali and B.P. Gorman, *J. Lumin.* 128, 1641 (2008).
37. S. Monticone, R. Tufeu, and A.V. Kanaev, *J. Phys. Chem. B.* 102, 2854 (1998).
38. S. Baek, J. Song, and S. Lim, *Phys. B* 399, 101 (2007).
39. E.F. Keskenler, G. Turgut, and S. Doğan, *Superlattices Microstruct.* 52, 107 (2012).
40. H. Chen, W. Guo, J. Ding, and S. Ma, *Superlattices Microstruct.* 51, 544 (2012).
41. R.N. Gayen, A. Rajaram, R. Bhar, and A.K. Pal, *Thin Solid Films* 518, 1627 (2010).
42. A. Jakhar, A. Jamdagni, A. Bakshi, T. Verma, V. Shukla, P. Jain, N. Sinha, and P. Arun, *Solid State Commun.* 168, 31 (2013).
43. J.I. Pankove, *Optical Processes in Semiconductors* (Englewoord Cliffs: Prentice-Hall Inc, 1971).
44. T. Ghosh, M. Dutta, S. Mridha, and D. Basak, *J. Electrochem. Soc.* 156, H285 (2009).
45. A.P. Roth, J.B. Webb, and D.F. Williams, *Solid State Commun.* 39, 1269 (1981).
46. K.A. Jeon, J.H. Kim, W.Y. Shim, W.Y. Lee, M.H. Jung, and S.Y. Lee, *J. Cryst. Growth* 287, 66 (2006).
47. F. Urbach, *Phys. Rev.* 92, 1324 (1953).
48. Y. Chen, X.L. Xu, G.H. Zhang, H. Xue, and S.Y. Ma, *Phys. B* 404, 3645 (2009).
49. A. Sayed, S. Taha, G. Said, A.A. Al-Ghamdi, and F. Yakuphanoglu, *Superlattices Microstruct.* 60, 108 (2013).
50. A.-S. Gadallah and M.M. El-Nahass, *Adv. Condens. Matter Phys.* 2013, 11 (2013).
51. M. DrDomenico Jr. and S.H. Wemple, *J. Appl. Phys.* 40, 720 (1969).
52. H. Benzarouk, A. Drici, M. Mekhnache, A. Amara, M. Guerioune, J.C. Bernède, and H. Bendjffal, *Superlattices Microstruct.* 52, 594 (2012).
53. M. Frumar, J. Jedelský, B. Frumarova, T. Wagner, and M. Hrdlička, *J. Non-Cryst. Solids* 326, 399 (2003).
54. H. Ticha and L. Tichy, *J. Optoelectron. Adv. Mater.* 4, 381 (2002).
55. C.C. Wang, *Phys Rev B* 2, 2045 (1970).
56. J.J. Wynne, *Phys. Rev. Lett.* 29, 650 (1972).
57. H. Nasu and J.D. Mackenzie, *Opt. Eng.* 26, 262102 (1987).
58. R. Adair, L.L. Chase, and S.A. Payne, *Phys. Rev. B* 39, 3337 (1989).
59. D. Hanna, *J. Mod. Opt.* 35, 12 (1988).
60. E.R. Shaaban, M. El-Hagary, H.S. Hassan, Y.A. Ismail, M. Emam-Ismail, and A.S. Ali, *Appl. Phys. A* 122, 1 (2016).
61. M. Ajili, M. Castagne, and N.K. Turki, *Superlattices Microstruct.* 53, 213 (2013).